

Control of Oscillations in Flow Problems under Frequency Limitations

COŞKU KASNAKOĞLU

Department of Electrical and Electronics Engineering TOBB University of Economics and Technology 06560 Ankara, Turkey (kasnakoglu@etu.edu.tr)

(Received ; accepted 11 August 2009)

Abstract: In this paper we investigate the control of flow problems where the control objective is to reduce the oscillation amplitude while keeping the frequency of oscillation between predefined limits at all times. The governing equations are simplified to obtain the oscillatory mode dynamics, after which the conditions that the control parameters must satisfy in order to achieve the desired objective are derived in detail. The results obtained are illustrated on a physical application example, namely cavity flow control, where it is seen that the controller is successful in achieving the control goal.

Key words: fluid flow, flow control, frequency limits, cavity flow.

1. INTRODUCTION

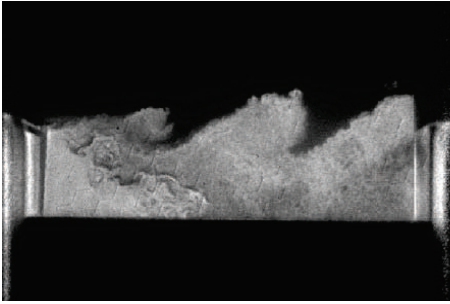
Fluid flow can be defined as the motion of liquids or gases, which is a phenomenon that one encounters continuously in everyday life. The flow of air around the body of a car or the wing of an aircraft, the motion of petroleum through pipelines, flow of water in oceans, and the motion of air in the atmosphere carrying the clouds are a few examples of fluid flows. Flow control refers to the ability to manipulate fluid flow in order to achieve a desired change in its behavior. Flow control is very important from a technological point of view and offers many potential benefits, such as reducing fuel costs for land, air, and sea vehicles, and improving effectiveness of industrial processes (Gad-el Hak, 2000). As such, flow control has received significant attention from multiple disciplines, and the interdisciplinary nature of its problems still presents unique challenges to the researcher (Bewley, 2001). Among a myriad of research on the topic one can find studies of flow control in aircraft and airfoils (Joslin, 1998; Wu et al., 1998), control of channel flows (Cortelezzi et al., 1998; Hogberg et al., 2001; Aamo et al., 2003; Baramov et al., 2004), control of turbulent boundary layers (Kim, 2003), control of combustion instability (Banaszuk et al., 2004), stabilization of bluff-body flow (Cohen et al., 2005), control of cylinder wakes (Noack and Eckelmann, 1994; Noack et al., 2003, 2005), control of cavity flows (Rowley and Marsden, 2000; Rowley et al., 2004; Fitzpatrick et al., 2005; Samimy et al., 2007; Caraballo et al., 2007), optimal control of vortex shed-

ding (Graham et al., 1999; Singh et al., 2001), and control of fluid flow in capillaries (Seiler et al., 1994; Oleschuk et al., 2000).

Most flow applications are modeled by the Navier–Stokes (NS) equations, or their simplified form Burgers’ equations, so studies of these equations are of interest (Krstic, 1999; Park and Lee, 2000; Kobayashi and Oya, 2003; Hinze and Kunisch, 2004; Smaoui, 2005). Although Navier–Stokes equations describe the flow behavior very accurately, a direct analysis of these equations is often quite difficult and for systematic control system design it is preferable to obtain reduced-order control-oriented models approximating the Navier–Stokes equations. A common approach is to utilize the POD/GP method, where one constructs an energy-optimal set of basis vectors for the flow via proper orthogonal decomposition (POD), and projects the NS equations onto the space spanned by the POD basis via Galerkin projection (GP) to obtain a finite-dimensional system of differential equations (Sirovich, 1987; Holmes et al., 1996). POD/GP methods have been used to develop controls for flow applications, including feedback control of cylinder wakes (Noack and Eckelmann, 1994; Noack et al., 2003, 2005), control of cavity flows (Rowley and Marsden, 2000; Rowley et al., 2004; Fitzpatrick et al., 2005; Samimy et al., 2007; Caraballo et al., 2007), and optimal control of vortex shedding (Singh et al., 2001). Also worth mentioning are input-separation (IS) techniques, which are important extensions to POD/GP (Efe and Ozbay, 2004; Camphouse, 2005; Kasnakoglu and Serrani, 2007). These methods address the problem that the control input gets embedded into the Galerkin system coefficients, and remedy the issue by producing stand-alone control terms in the dynamics. Models produced by POD/GP/IS approaches can be further simplified for problems that exhibit oscillatory limiting behavior, by the use an appropriate *ansatz* to obtain the dynamics of the oscillatory modes (Landau and Lifshitz, 1987; Noack et al., 2003; Stuart, 2006).

In this paper we study the suppression of unwanted oscillations in fluid flow problems, utilizing a model obtained by the aforementioned reduction strategies. The control design is subject to the constraint that the frequency of oscillation must be kept between certain limits at all times. Such a constraint is important in real-life problems for various reasons. For instance, many actuators are unable to produce excitations and many transducers are unable to take measurements outside a certain frequency range. An example is synthetic jet actuators, which are of the most commonly used actuators in flow control (Amitay et al., 2001; Gilaranz et al., 2005; Caraballo et al., 2007; Samimy et al., 2007). Synthetic jet actuators operate by moving a membrane or diaphragm up and down, sucking the surrounding fluid into a chamber and then expelling it. The lack of an external source for the fluid makes it necessary that the device keep vibrating to sustain its operation. Hence, the flow must remain oscillatory at all times so that a feedback controller can be implemented through these devices. Similar arguments can be made for the transducers used for measurements. It is therefore of practical importance to obtain a control design that will be able to reduce the amplitude of the unwanted oscillation, while at the same keeping the oscillation frequency within desired limits, which is the main topic of this paper.

The paper is organized as follows: Section 2 introduces and describes the problem. Section 3 presents the main results, which are the conditions under which the oscillation amplitude can be suppressed while maintaining the frequency within a desired range at all times. Section 4 demonstrates the application of the results to a real-life flow control problem, namely the control of unwanted oscillations resulting from air flow past a cavity. Section 5 concludes the paper with final discussions and future work ideas.



(a) Flow over a shallow cavity (figure courtesy of OSU GDTL)



(b) Flow around a circular cylinder (figure courtesy of ONERA)

Figure 1. Two examples of real-life flow configurations with self-sustained oscillations.

2. PROBLEM DESCRIPTION

Fluid flow processes are most commonly described by the Navier–Stokes partial differential equations (PDEs). We shall consider the flow to be isentropic to simplify the final form of the system. With this treatment, it was shown by Rowley et al. (2004) that the compressible Navier–Stokes equations can be written as¹

$$\frac{D\mathbf{u}}{Dt} + \frac{1}{M^2} \frac{2}{\kappa - 1} \nabla c = \frac{1}{\text{Re}} \nabla^2 \mathbf{u}, \quad (1)$$

$$\frac{Dc}{Dt} + \frac{\kappa - 1}{2} c \operatorname{div} \mathbf{u} = 0, \quad (2)$$

where $\mathbf{u}(\mathbf{x}, t) = (u_s(\mathbf{x}, t), u_n(\mathbf{x}, t))$ is the flow velocity in the stream-wise and normal directions, $c(\mathbf{x}, t)$ is the local speed of sound, the operator $D/Dt = \partial/\partial t + \mathbf{u} \cdot \nabla$ stands for the material derivative, and $\mathbf{x} = (x, y)$ denotes Cartesian coordinates over the spatial domain $\Omega \subset \mathbb{R}^2$. The constants κ , Re , and M denote respectively ratio of specific heats, Reynolds number, and Mach number. The Navier–Stokes equations 1–2 are subject to some initial conditions and boundary conditions, and the system input $\gamma \in \mathbb{R} \rightarrow \mathbb{R}$ affects the system through the latter. Also, let $\mathbb{H} = \mathcal{L}_2(\Omega, \mathbb{R}^3)$ be the square-integrable functions on Ω , where $\mathbf{q} := (u_s - u_{s0}, u_n - u_{n0}, c - c_0) \in \mathbb{H}$ is the fluctuations of the flow velocity about the mean value $\mathbf{q}_0 = (u_{n0}, u_{s0}, c_0)$. In this paper we shall focus our attention to flows that exhibit an undesired oscillation in the absence of a control action. Examples of such flows include the flow over a shallow cavity and the flow around a circular cylinder, which are shown in Figure 1. The goal is to find the control law γ so that the oscillation amplitude is reduced, while the frequency of oscillation is kept between desired limits at all times.

To perform the design directly on the Navier–Stokes equations 1–2 is very difficult, if not impossible, due to the complicated and infinite-dimensional nature of these PDEs. Therefore, we shall first look for a way to simplify these equations. A common approach for the simplification of the Navier–Stokes equations is to employ proper orthogonal decomposi-

tion (POD) followed by Galerkin projection (GP) (Sirovich, 1987; Holmes et al., 1996). In this approach one first obtains a set of POD modes for this system denoted by $\{q_i(x)\}_{i=0}^N$. These POD modes are orthonormal, i.e. $(q_i, q_j)_\Omega = \delta_{ij}$, and the inner product is defined as $(u, v) := \int_\Omega u \cdot v \, dV$. Projecting the velocity vector \mathbf{q} onto these modes, one obtains the POD expansion as

$$\mathbf{q}(x, t) \approx \mathbf{q}^{[N]}(x, t) = \mathbf{q}_0(x) + \sum_{i=1}^N a_i(t) q_i(x). \quad (3)$$

The coefficients $a_i(t)$ are called *POD coefficients* and they capture the time dependence. Equation 3 is then substituted into equations 1–2 to obtain the dynamics in terms of the time coefficients $\{a_i(t)\}_{i=0}^N$. Following a shift by the equilibrium point, this procedure yields a set of N differential equations

$$\dot{a}_i = \frac{1}{Re} \sum_{j=1}^N l_{ij} a_j + \sum_{j,k=1}^N q_{ijk} a_j a_k, \quad (4)$$

where l_{ij} and q_{ijk} are the Galerkin system coefficients. System 4 can be expressed in compact form as

$$\dot{a} = La + Q(a, a), \quad (5)$$

where $a = \{a_i\}_{i=1}^N \in \mathbb{R}^N$, $\gamma \in \mathbb{R}$, $L = \{l_{ij}\}_{i,j=1}^N \in \mathbb{R}^{N \times N}$, $Q(a) = \{a^T Q_i a\}_{i=1}^N \in \mathbb{R}^N$, $Q_i = \{q_{ijk}\}_{j,k=1}^N \in \mathbb{R}^{N \times N}$. Note that the effect of the system input γ is not directly visible in 4 and 5 as it gets embedded into the Galerkin system coefficients l_{ij} and q_{ijk} . Techniques for input separation (IS) such as those of Camphouse (2005), Efe and Ozbay (2004), and Kasnakoglu et al. (2008) have been devised to remedy this situation, which make the control input γ appear explicitly through linear, quadratic, and/or bilinear terms in the Galerkin system equations. We shall consider the case in which the input terms are linear to simplify the analysis, which yields a Galerkin system of the form

$$\dot{a} = La + Q(a, a) + B\gamma, \quad (6)$$

where $B = \{b_i\}_{i=1}^N \in \mathbb{R}^N$. The Galerkin system can be further simplified using a Kryloff–Bogoliubov (KB) *ansatz* of the form $a_1 = r \cos \omega t$, $a_2 = r \sin \omega t$, and $a_i = k_i$ for $i \geq 3$ (Jordan and Smith, 1999; Noack et al., 2003). Here, a_1 and a_2 are the *oscillatory modes*, a_i for $i \geq 3$ are the *shift modes*, $r^2 := a_1^2 + a_2^2$, $\theta := \arctan(a_2/a_1) = \omega t$, and $k_i \in \mathbb{R}_+$. Utilizing mean-field models, invariant manifold reduction, or center-manifold theory, it can be shown that the shift-mode amplitudes k_i are locally slaved to the oscillation amplitude r (Noack et al., 2003; Kasnakoglu and Serrani, 2007). Using this dependence to eliminate the shift modes from the equations, and utilizing the KB *ansatz*, one arrives at the simplified evolution equation for the oscillatory modes as

$$\frac{\partial a_1}{\partial t} = \sigma a_1 - \omega a_2 - \alpha a_1^3 - \alpha a_2^2 + b_1 \gamma, \quad (7)$$

$$\frac{\partial a_2}{\partial t} = \omega a_1 + \sigma a_2 - \alpha a_1^2 - \alpha a_2^3 + b_2 \gamma, \quad (8)$$

where $\sigma, \alpha, \omega \in \mathbb{R}_+$ are functions of the Galerkin system coefficients l_{ij} and q_{ijk} . Expressed in polar coordinates (r, θ) , the system 7–8 becomes

$$\dot{r} = \sigma r - \alpha r^3 + (b_1 \cos(\theta) + b_2 \sin(\theta))\gamma, \quad (9)$$

$$\dot{\theta} = \omega + \frac{1}{r}(b_2 \cos(\theta) - b_1 \sin(\theta))\gamma. \quad (10)$$

A natural choice for the control law γ in oscillatory fluid flow problems is to apply a sinusoidal signal whose amplitude and phase are varied based on the system states, i.e.

$$\gamma(t) = Ar(t) \cos(\theta(t) - \phi), \quad (11)$$

where $A \in \mathbb{R}$, $\phi \in [0, 2\pi]$ are controller parameters to be determined. Substituting equation 11 into equations 9–10 yields

$$\dot{r} = (\sigma + A(\cos(\theta)b_1 + \sin(\theta)b_2)(\cos(\phi)\cos(\theta) + \sin(\phi)\sin(\theta)))r - \alpha r^3, \quad (12)$$

$$\dot{\theta} = \omega + A(\cos(\theta)b_2 - \sin(\theta)b_1)(\cos(\phi)\cos(\theta) + \sin(\phi)\sin(\theta)). \quad (13)$$

The goal is to determine the control parameters A and ϕ such that the following two criteria are satisfied:

Criterion 2.1 (Frequency criterion). The oscillation frequency remains within predefined design limits at all times, i.e. given $\omega_{\text{low}}, \omega_{\text{high}}$ such that $0 < \omega_{\text{low}} < \omega < \omega_{\text{high}}$, we require that $\omega_{\text{low}} < \dot{\theta} < \omega_{\text{high}}$ for all $t > 0$.

Criterion 2.2 (Amplitude criterion). The oscillation amplitude tends to zero with time, i.e. $r \rightarrow 0$ as $t \rightarrow \infty$.

In the next section we will derive guidelines as to how the parameters A and ϕ can be selected to satisfy these criteria.

3. MAIN RESULTS

In this section we present the results regarding the selection of the control parameters so as to satisfy the design goals given in Criteria 2.1 and 2.2.

Theorem 3.1 (Frequency condition). *For the fluid flow problem described in Section 2, let $\omega_{\text{low}} \in \mathbb{R}_+$ and $\omega_{\text{high}} \in \mathbb{R}_+$ be the lower and upper bounds of the allowable frequency range of oscillation, where $0 < \omega_{\text{low}} < \omega < \omega_{\text{high}}$. A control law of the form $\gamma = A^* r \cos(\theta - \phi^*)$ will achieve*

$$\omega_{\text{low}} < \dot{\theta} < \omega_{\text{high}} \quad \forall t > 0 \quad (14)$$

if (ϕ^*, A^*) is an element of $\mathcal{S}_f \subset \mathbb{R}^2$, defined as

$$\mathcal{S}_f := \mathcal{S}_1 \cap \mathcal{S}_2, \quad (15)$$

where

$$\mathcal{S}_1 := \{(\phi, A) : A_1(\phi) < A < A_2(\phi)\}, \quad (16)$$

$$\mathcal{S}_2 := \{(\phi, A) : A'_1(\phi) < A < A'_2(\phi)\} \quad (17)$$

and

$$A_1(\phi) = \frac{2(\omega - \omega_{\text{low}}) \left(b_2 \cos(\phi) - b_1 \sin(\phi) - \sqrt{b_2^2 + b_1^2} \right)}{(b_1 \cos(\phi) + b_2 \sin(\phi))^2}, \quad (18)$$

$$A_2(\phi) = \frac{2(\omega - \omega_{\text{low}}) \left(b_2 \cos(\phi) - b_1 \sin(\phi) + \sqrt{b_2^2 + b_1^2} \right)}{(b_1 \cos(\phi) + b_2 \sin(\phi))^2}, \quad (19)$$

$$A'_1(\phi) = \frac{2(\omega - \omega_{\text{high}}) \left(b_2 \cos(\phi) - b_1 \sin(\phi) + \sqrt{b_2^2 + b_1^2} \right)}{(b_1 \cos(\phi) + b_2 \sin(\phi))^2}, \quad (20)$$

$$A'_2(\phi) = \frac{2(\omega - \omega_{\text{high}}) \left(b_2 \cos(\phi) - b_1 \sin(\phi) - \sqrt{b_2^2 + b_1^2} \right)}{(b_1 \cos(\phi) + b_2 \sin(\phi))^2}. \quad (21)$$

Proof. Let us first determine the conditions under which $\dot{\theta} > \omega_{\text{low}}$. Using the dynamics of θ from equations 12–13, we can write

$$\begin{aligned} \omega_{\text{low}} < \dot{\theta} &= \omega + A (\cos(\theta) b_2 - \sin(\theta) b_1) (\cos(\phi) \cos(\theta) + \sin(\phi) \sin(\theta)), \\ \omega_{\text{low}} - \omega < &Ab_2 \cos(\phi) \cos^2(\theta) - Ab_1 \sin(\phi) \sin^2(\theta) \\ &+ (Ab_2 \sin(\phi) - Ab_1 \cos(\phi)) \sin(\theta) \cos(\theta). \end{aligned}$$

Dividing both sides by $\cos^2(\theta)$ and using the identity $\cos^{-2}(\theta) = \sec^2(\theta) = 1 + \tan^2(\theta)$,

$$\begin{aligned} (1 + \tan^2(\theta))(\omega_{\text{low}} - \omega) < &Ab_2 \cos(\phi) + (Ab_2 \sin(\phi) - Ab_1 \cos(\phi)) \tan(\theta) \\ &- Ab_1 \sin(\phi) \tan^2(\theta). \end{aligned}$$

Expanding and collecting terms,

$$0 < (\omega - \omega_{\text{low}} - Ab_1 \sin(\phi)) \tan^2(\theta) + (Ab_2 \sin(\phi) - Ab_1 \cos(\phi)) \tan(\theta) \\ + Ab_2 \cos(\phi) + \omega - \omega_{\text{low}}.$$

The right-hand side of this equation is a quadratic polynomial in $\tan(\theta)$, which must always be positive for the inequality above to be satisfied. This can be achieved if the leading coefficient is positive and the discriminant Δ_1 is negative. The former requires that

$$(\omega - \omega_{\text{low}} - Ab_1 \sin(\phi)) > 0. \quad (22)$$

For the latter, the negativity condition of the discriminant Δ_1 can be written as

$$\Delta_1 = (Ab_2 \sin(\phi) - Ab_1 \cos(\phi))^2 - 4(\omega - \omega_{\text{low}} - Ab_1 \sin(\phi))(Ab_2 \cos(\phi) \\ + \omega - \omega_{\text{low}}) < 0,$$

$$\Delta_1 = (b_2 \sin(\phi) + b_1 \cos(\phi))^2 A^2 + (-4(\omega - \omega_{\text{low}})b_2 \cos(\phi) + 4b_1 \sin(\phi)(\omega - \omega_{\text{low}}))A \\ - 4(\omega - \omega_{\text{low}})^2 < 0.$$

The equation above for Δ_1 is quadratic in A with a positive leading coefficient $(b_2 \sin(\phi) + b_1 \cos(\phi))^2$. Therefore, it will be negative between its roots, which can be computed from the quadratic formula to be

$$A_1 = \frac{2(\omega - \omega_{\text{low}})(b_2 \cos(\phi) - b_1 \sin(\phi) - \sqrt{b_2^2 + b_1^2})}{(b_1 \cos(\phi) + b_2 \sin(\phi))^2}, \\ A_2 = \frac{2(\omega - \omega_{\text{low}})(b_2 \cos(\phi) - b_1 \sin(\phi) + \sqrt{b_2^2 + b_1^2})}{(b_1 \cos(\phi) + b_2 \sin(\phi))^2}.$$

Therefore, for a given (A^*, ϕ^*) , we will have $\dot{\theta} > \omega_{\text{low}}$ if (A^*, ϕ^*) satisfies equation 22, as well as $A_1(\phi^*) < A^* < A_2(\phi^*)$. If we let

$$\mathcal{S}_0 := \{(\phi, A) : \omega - \omega_{\text{low}} - Ab_1 \sin(\phi) > 0\},$$

$$\mathcal{S}_1 := \{(\phi, A) : A_1(\phi) < A < A_2(\phi)\},$$

then this is equivalent to saying that $(\phi^*, A^*) \in \mathcal{S}_0 \cap \mathcal{S}_1$. It can also be shown that $\mathcal{S}_1 \subset \mathcal{S}_0$ (see Lemma A.1), so the condition for $\dot{\theta} > \omega_{\text{low}}$ becomes $(\phi^*, A^*) \in \mathcal{S}_1$. The conditions for $\dot{\theta} < \omega_{\text{high}}$ can be obtained similarly to be $(A^*, \phi^*) \in \mathcal{S}'_0 \cap \mathcal{S}_2$, where

$$\mathcal{S}'_0 := \{(\phi, A) : \omega - \omega_{\text{high}} - Ab_1 \sin(\phi) < 0\},$$

$$\mathcal{S}_2 := \{(\phi, A) : A'_1(\phi) < A < A'_2(\phi)\}$$

and

$$A'_1 = \frac{2(\omega - \omega_{\text{high}})(b_2 \cos(\phi) - b_1 \sin(\phi) + \sqrt{b_2^2 + b_1^2})}{(b_1 \cos(\phi) + b_2 \sin(\phi))^2},$$

$$A'_2 = \frac{2(\omega - \omega_{\text{high}})(b_2 \cos(\phi) - b_1 \sin(\phi) - \sqrt{b_2^2 + b_1^2})}{(b_1 \cos(\phi) + b_2 \sin(\phi))^2}.$$

In addition, it can be proved that $\mathcal{S}_2 \subset \mathcal{S}'_0$ (see Lemma A.3), so the condition for $\dot{\theta} < \omega_{\text{high}}$ becomes $(A^*, \phi) \in \mathcal{S}_2$. Collecting the results for the $\dot{\theta} > \omega_{\text{low}}$ and $\dot{\theta} < \omega_{\text{high}}$ cases above, the condition for the frequency criterion becomes $(\phi^*, A^*) \in \mathcal{S}_1 \cap \mathcal{S}_2$, which is the statement of the theorem. \square

Theorem 3.2 (Magnitude condition). *For the fluid flow problem described in Section 2, a control law of the form $\gamma = A^* r \cos(\theta - \phi^*)$, where $(\phi^*, A^*) \in \mathcal{S}_f$ with \mathcal{S}_f as given in equation 15, will achieve*

$$r \rightarrow 0 \quad \text{as} \quad t \rightarrow \infty \quad (23)$$

if

$$(\phi^*, A^*) \in \mathcal{S}_m, \quad (24)$$

where

$$\mathcal{S}_m := \{(\phi, A) : 1/2 Ab_1 \cos(\phi) + \sigma + 1/2 Ab_2 \sin(\phi) < 0\}. \quad (25)$$

Proof. We first rewrite the controlled system in polar form given in equations 12–13 compactly as follows:

$$\dot{r} = g(\theta, \phi, A)r - \alpha r^3, \quad (26)$$

$$\dot{\theta} = h(\theta, \phi, A), \quad (27)$$

where

$$g(\theta, \phi, A) := \sigma + (\cos(\theta)b_1 + \sin(\theta)b_2)A(\cos(\phi)\cos(\theta) + \sin(\phi)\sin(\theta)),$$

$$h(\theta, \phi, A) := \omega + (\cos(\theta)b_2 - \sin(\theta)b_1)A(\cos(\phi)\cos(\theta) + \sin(\phi)\sin(\theta)).$$

Since the control parameters A and ϕ are selected such that $(\phi, A) \in \mathcal{S}$, we have $0 < \omega_{\text{low}} < \dot{\theta} < \omega_{\text{high}}$, so $\dot{\theta}$ is always positive, which means that θ is strictly increasing in time. Therefore, one can map time values t to angle values θ with a one to one and onto function χ such that

$$\theta = \chi(t) \quad \text{and} \quad t = \chi^{-1}(\theta), \quad (28)$$

where χ is the solution of equation 27 starting from $\theta(0) = \theta_0$. This one to one and onto correspondence makes it meaningful to view θ as a new time scale instead of t , and investigate the dynamics of r with respect to θ , which is

$$\frac{dr}{d\theta} = \frac{dr}{dt} \frac{dt}{d\theta} = \frac{\dot{r}}{\dot{\theta}} = \frac{(g(\theta, \phi, A)r - \alpha r^3)}{\dot{\theta}}.$$

Since $0 < \omega_{\text{low}} < \dot{\theta} < \omega_{\text{high}}$, one can write

$$\omega_{\text{high}}^{-1} (g(\theta, \phi, A)r - \alpha r^3) < \frac{dr}{d\theta} < \omega_{\text{low}}^{-1} (g(\theta, \phi, A)r - \alpha r^3).$$

It therefore makes sense to analyze the following two systems:

$$\Sigma_1 : \frac{dr}{d\theta} = \omega_{\text{high}}^{-1} (g(\theta, \phi, A)r - \alpha r^3), \quad (29)$$

$$\Sigma_2 : \frac{dr}{d\theta} = \omega_{\text{low}}^{-1} (g(\theta, \phi, A)r - \alpha r^3) \quad (30)$$

as they provide bounds for the behavior of the original system. Let us start with system Σ_1 in equation 29 and divide by r^3 to get

$$\frac{1}{r^n} \frac{dr}{d\theta} = \omega_{\text{high}}^{-1} \left(g(\theta, \phi, A) \frac{1}{r^2} - \alpha \right). \quad (31)$$

Defining a change of variable $s := 1/r^2$, differentiating, and substituting into equation 31 above,

$$-\frac{1}{2} \frac{ds}{d\theta} = \omega_{\text{high}}^{-1} (g(\theta, \phi, A)s - \alpha). \quad (32)$$

Defining

$$M(\theta, \phi, A) := e^{2\omega_{\text{high}}^{-1} \int_0^\theta g(z, \phi, A) dz},$$

multiplying both sides of equation 32 by $M(\theta)$, rearranging, and collecting terms yields

$$\frac{d}{d\theta} (sM(\theta, \phi, A)) = 2\omega_{\text{high}}^{-1} M(\theta, \phi, A)\alpha.$$

Integrating both sides results in

$$\int_0^\theta \frac{d}{dy} (sM(y, \phi, A)) dy = \int_0^\theta 2\omega_{\text{high}}^{-1} M(y, \phi, A)\alpha dy,$$

$$sM(\theta, \phi, A) - s(0)M(0, \phi, A) = 2\omega_{\text{high}}^{-1} \alpha \int_0^\theta M(y, \phi, A) dy.$$

Transforming from s back to r , rearranging, and solving for r yields

$$r(\theta)^2 = \frac{M(\theta, \phi, A)r_0^2}{2\omega_{\text{high}}^{-1}r_0^2\alpha \int_0^\theta M(y, \phi, A)dy + 1}. \quad (33)$$

If the control parameters are selected such that $(\phi^*, A^*) \in \mathcal{S}_m$, then it can be shown (Lemma A.4) that as $\theta \rightarrow \infty$, $M(\theta, \phi^*, A^*) \rightarrow 0$ and $0 < C_4 \leq \lim_{\theta \rightarrow \infty} \int_0^\theta M(y, \phi, A)dy \leq C_5$ for some $C_4, C_5 \in \mathbb{R}_+$. Therefore, we see from equation 33 that $r \rightarrow 0$ as $\theta \rightarrow \infty$. The same result can be obtained for system Σ_2 in equation 30 in a similar fashion. Since the trajectories of Σ_1 and Σ_2 bound the trajectories of the original system from above and below, it follows that $r \rightarrow 0$ as $\theta \rightarrow \infty$ for the original system as well. Since $\theta = \chi(t)$, where χ is monotonically increasing, we conclude that $r \rightarrow 0$ as $t \rightarrow \infty$, which is the statement of the theorem. \square

Remark 3.3. The careful reader might notice that the condition 25 is consistent with those that can be obtained by phase-averaging techniques. However, there are important subtle points about the phase-averaging approach that can be identified using the main results above. We shall not elaborate further on this issue at this point so as not to deviate from the main discussion, but we provide some comments in Appendix B for the interested reader.

4. APPLICATION EXAMPLE: CAVITY FLOW CONTROL

In this section a physical flow control problem, namely the suppression of unwanted oscillations generated by the air flow over a shallow cavity, is considered as an example. As mentioned in the introduction, this is a problem that has captured significant research interest (Rowley and Marsden, 2000; Rowley et al., 2004; Fitzpatrick et al., 2005; Caraballo et al., 2007; Samimy et al., 2007) and has been the initial motivation for this study. Air flowing over a shallow cavity exhibits a strong self-sustained resonance caused by a natural feedback mechanism. Acoustic waves are scattered by shear-layer structures impacting the trailing edge of the cavity. These acoustic waves travel upstream to reach the receptivity region of the shear layer, where they tune and enhance the development and growth of shear-layer structures. The resulting acoustic fluctuations can be very intense and are known to cause, among other problems, store damage and airframe structural fatigue in weapons bay applications. To suppress or reduce the pressure fluctuations inside the cavity, feedback control is applied to the flow by using a synthetic jet-like actuator, which is typically an acoustic actuator located at the cavity trailing edge (Samimy et al., 2007). A schematic representation is illustrated in Figure 2. As described in Section 2, we first start with the Navier–Stokes PDEs governing the flow process and obtain a Galerkin system describing the flow. For this purpose we utilize the system parameters from the study Samimy et al. (2007) and take $N = 20$ for the order of the Galerkin system. This allows the Galerkin system to capture a sufficient amount of energy to produce a faithful representation of the flow. Proceeding with further reduction utilizing a KB *ansatz*, we arrive at the oscillatory mode dynamics 9–10, with the parameter values given as $\sigma = 0.1368$, $\alpha = 0.2790$, $\omega = 2.5133$, $b_1 = -7.6412 \times 10^{-4}$, and $b_2 = -1.1000 \times 10^{-4}$. The unforced response of the oscillation mode dynamics is given in Figure 3 and the response of the high-order Galerkin model is given in Figure 4 for comparison. In Figure 4, only the first four modes of the Galerkin system are plotted as plotting all 20 would produce clutter. It is seen that the oscillatory mode dynamics adequately represent key

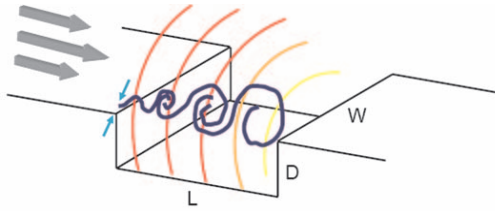


Figure 2. Control of cavity flow oscillations using actuation at the cavity trailing edge (figure courtesy of OSU GDTL).

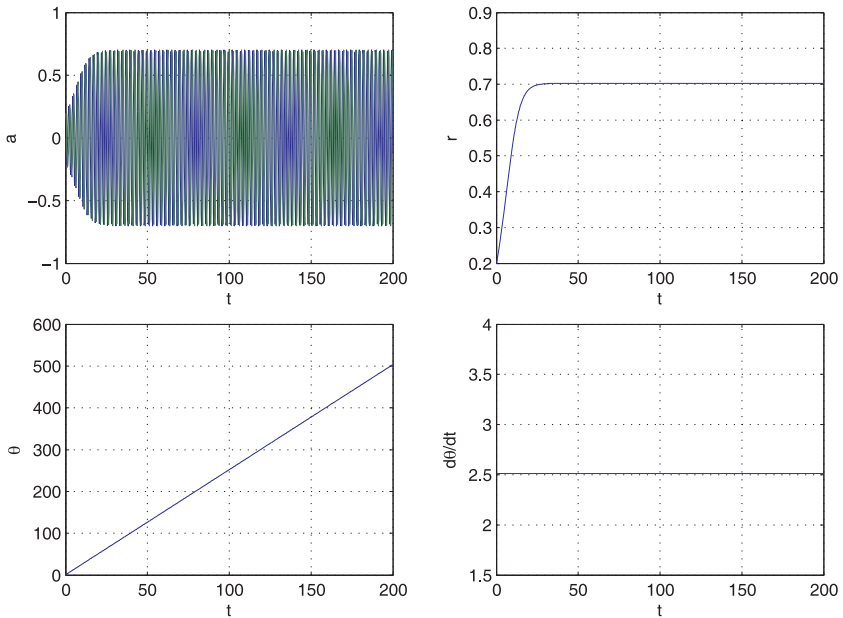


Figure 3. Unforced response of the oscillatory mode dynamics.

trends and qualities of the response, such as the rise time, oscillation amplitude, and oscillation frequency, and the quantitative values produced by the simple model are also reasonable. For the control design, we set the frequency limits to be $\omega_{\text{low}} = 2.14$ and $\omega_{\text{high}} = 2.89$, which allows a frequency change of about 15% from ω in both directions. The curves in the (ϕ, A) plane corresponding to the frequency constraints as given in Theorem 3.1 and the curves corresponding to the magnitude condition as given in Theorem 3.2 are plotted in Figure 5.

The red zone is where the frequency criterion is satisfied, and the green zone is where the magnitude criterion is satisfied. The control parameters we seek are those that will result in a response satisfying both criteria, which corresponds to the intersection of the zones, which appears as brown in the figure.² The point $(\phi, A) = (54^\circ, 300)$, which is marked with a circle in the figure, lies in this region and we can therefore use these parameter values for the control law, i.e. $\gamma = 300r \cos(\theta - 54\pi/180)$. Figure 6 shows the closed-loop response of the oscillation modes, where the controller is turned on at $t = 50$ s. Figure 7 shows the

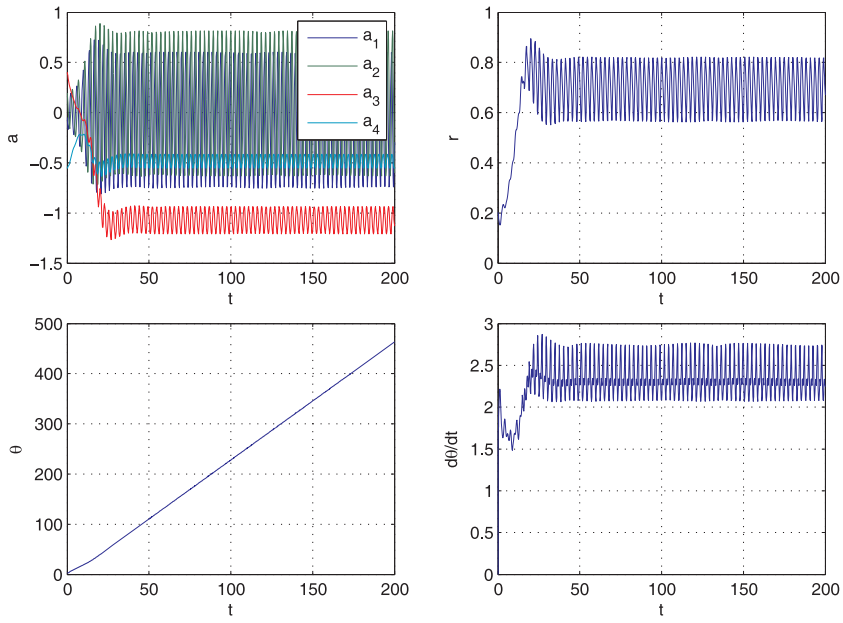


Figure 4. Unforced response of the high-order Galerkin model.

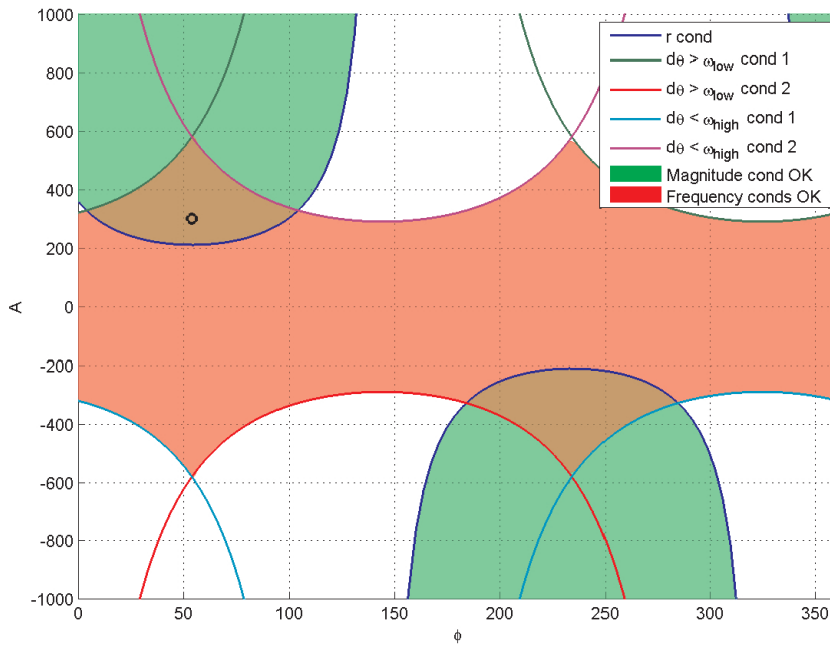


Figure 5. Frequency and magnitude conditions for controller parameter values A and ϕ .

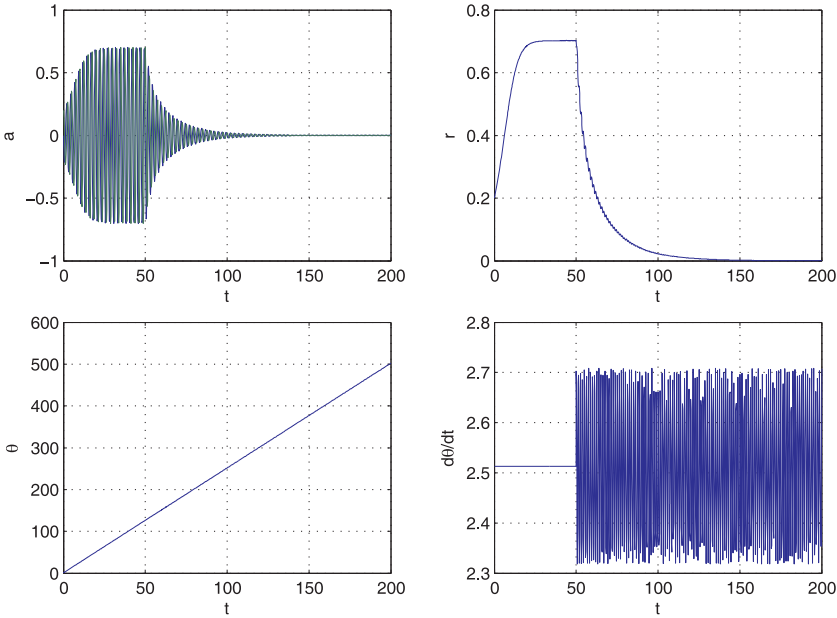


Figure 6. Controlled response of the oscillatory modes.

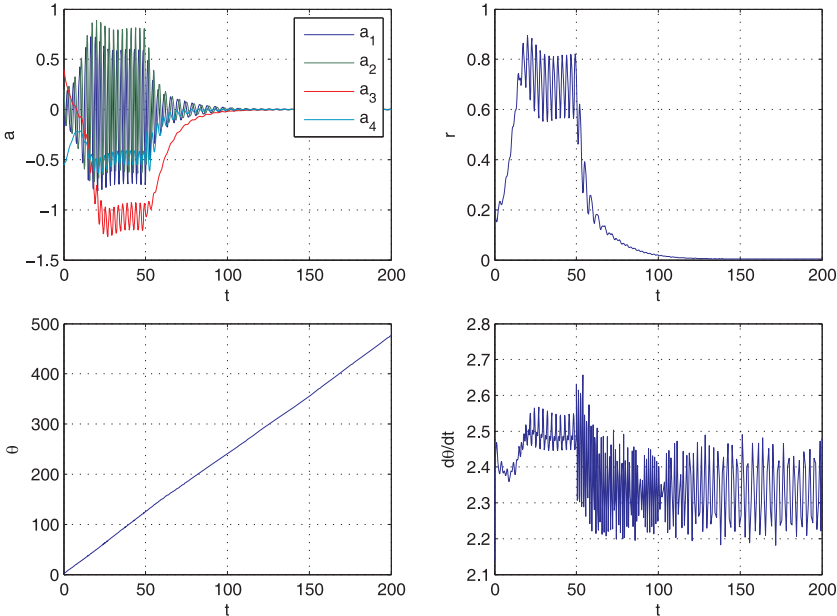


Figure 7. Controlled response of the high-order Galerkin model.

corresponding response for the high-order Galerkin model. It can be seen that the controller designed according to the simplified model, and then applied to the high-order Galerkin system accurately representing the cavity flow, achieves the desired task and drives $r \rightarrow 0$, in addition to keeping $\dot{\theta}$ between $\omega_{\text{low}} = 2.14$ and $\omega_{\text{high}} = 2.89$. Note also the similarity in behavior between the low-order model and the higher-order Galerkin system, especially in r , which is a further encouragement. There are inevitably some differences; for instance, the response of the frequency $\dot{\theta}$ in the higher-order Galerkin model shows some deviation from that of the simplified low-order model. Still, the approximation is good enough and the control law succeeds in achieving the desired objectives.

5. CONCLUSIONS AND FUTURE WORK

In this paper we studied the control of fluid flow problems where the control goal is to reduce the amplitude of undesired oscillations. This goal is to be realized under the constraint that the oscillation frequency must remain within a certain range at all times. A simplified model of the oscillatory modes was obtained from the flow dynamics, and rules for selecting the controller parameters achieving the desired objectives were derived. Cavity flow control was studied as a real-life example to illustrate the ideas developed. It was seen that the controller designed using the results developed in the paper was successful in suppressing cavity oscillations, while at the same time keeping the frequency within desired limits.

The problem studied in the paper is of practical importance, since many fluid flow configurations exhibit unwanted oscillations that need to be suppressed. However, most of the devices used for actuation and measurement can only operate within certain frequency limits, so they cannot physically realize arbitrary control laws. The results of the paper can provide guidelines to reducing unwanted oscillations through control laws that are actually realizable through such actuators and transducers.

Future work ideas and research directions include extending the ideas to different types of control laws and applying the results to different problems in flow control or possibly in other fields.

Acknowledgements. We would like to greatly acknowledge Professors Andrea Serrani and Mo Samimy and all members of the OSU GDTL Flow Control Group for our collaborative works on cavity flow control. We would also like to thank Professors Bernd Noack and Gilead Tadmor for fruitful and insightful discussions during the initial phases of our research.

APPENDICES

A. Auxiliary Lemmas

Below we present some auxiliary lemmas used for the derivation of the main results in Section 3.

Lemma A.1. *Let $\omega_{\text{low}} \in \mathbb{R}_+$ such that $0 < \omega_{\text{low}} < \omega$, and let*

$$\mathcal{S}_0 := \{(\phi, A) : \omega - \omega_{\text{low}} - Ab_1 \sin(\phi) > 0\},$$

$$\mathcal{S}_1 := \{(\phi, A) : A_1(\phi) < A < A_2(\phi)\},$$

where

$$A_1(\phi) = \frac{2(\omega - \omega_{\text{low}}) \left(b_2 \cos(\phi) - b_1 \sin(\phi) - \sqrt{b_2^2 + b_1^2} \right)}{(b_1 \cos(\phi) + b_2 \sin(\phi))^2},$$

$$A_2(\phi) = \frac{2(\omega - \omega_{\text{low}}) \left(b_2 \cos(\phi) - b_1 \sin(\phi) + \sqrt{b_2^2 + b_1^2} \right)}{(b_1 \cos(\phi) + b_2 \sin(\phi))^2}.$$

Then

$$\mathcal{S}_1 \subset \mathcal{S}_0.$$

Proof. For the sake of compactness, we will only give the proof for the case $b_1 > 0, b_2 > 0$. Proofs for other cases can be constructed similarly.

First, we assume that $\sin(\phi) > 0$, i.e. $0 < \phi < \pi$, without loss of generality. This is because if $\pi < \phi < 2\pi$ then the control $\gamma = A \cos(\theta - \phi)$ is equivalent to $\gamma = -A \cos(\theta - \phi')$, where $\phi' := \phi - \pi$ and hence $0 < \phi' < \pi$.

Note that for the case under consideration, $(\phi^*, A^*) \in \mathcal{S}_0 \iff A^* < A_0(\phi^*)$, where

$$A_0(\phi) := \frac{\omega - \omega_{\text{low}}}{b_1 \sin(\phi)}.$$

Define

$$B(\phi) := \frac{A_0(\phi)}{A_2(\phi)} = \frac{(b_1 \cos(\phi) + b_2 \sin(\phi))^2}{2 b_1 \sin(\phi) (b_2 \cos(\phi) - b_1 \sin(\phi) + \sqrt{b_2^2 + b_1^2})}.$$

Letting $x := \tan(\phi)$, $\sin(\phi) = x/\sqrt{1+x^2}$, and $\cos(\phi) = 1/\sqrt{1+x^2}$ and rearranging yields

$$B'(x) = 1/2 \frac{2 b_1 x b_2 + b_2^2 x^2 + b_1^2}{b_1 x \left(-b_1 x + b_2 + \sqrt{b_2^2 + b_1^2} \sqrt{1+x^2} \right)}. \quad (34)$$

Differentiating with respect to x and setting $\frac{dB'}{dx}(x) = 0$ yields

$$(1+x^2) = \frac{(x b_2 - 2 x^2 b_1 - b_1)^2 (b_2^2 + b_1^2)}{(2 b_1^2 x + b_2^2 x - b_2 b_1)^2}.$$

Rearranging gives

$$(x b_2 - b_1) (b_1 + x b_2)^3 = 0,$$

the roots of which are

$$\left\{ x_1 = \frac{b_1}{b_2}, x_2 = -\frac{b_1}{b_2}, x_3 = -\frac{b_1}{b_2}, x_4 = -\frac{b_1}{b_2} \right\}.$$

For $b_1, b_2 > 0$, we have $-b_1/b_2 < 0 < b_1/b_2$ and it can be shown that $\lim_{x \rightarrow 0} \frac{dB'}{dx}(x) = -\infty$. Hence, B' has only one local minimum, which occurs at $x_1 = b_1/b_2$, and which can be evaluated from equation 34 to be

$$B'(x_1) = B'(b_1/b_2) = 1.$$

Since we are considering the range $0 < \phi < \pi$, at the edges of this range we have $x_e = \tan(0+) = \tan(\pi-) = 0+$, for which one can show that $\lim_{x \rightarrow 0+} B'(x) = \infty > B'(x_1) = 1$. Thus, $B'(x_1)$ is the minimum for B' for the $b_1 > 0, b_2 > 0, 0 < \phi < \pi$ case being considered here. Therefore,

$$B(\phi) = \frac{A_0(\phi)}{A_2(\phi)} \geq \min_{\phi} B(\phi) = \min_x B'(x) = B'(b_1/b_2) = 1.$$

Since $A_2(\phi) > 0$, this implies that

$$A_0(\phi) \geq A_2(\phi).$$

Therefore,

$$(\phi^*, A^*) \in \mathcal{S}_1 \implies A^* < A_2(\phi^*) \leq A_0(\phi^*) \implies A^* < A_0(\phi) \implies (\phi^*, A^*) \in \mathcal{S}_0,$$

which shows that $\mathcal{S}_1 \subset \mathcal{S}_0$. □

Remark A.2. As indicated in the beginning of the proof above, we only considered the case $b_1 > 0, b_2 > 0$ for the sake of compactness. The proofs for other cases can be considered in a similar manner. For instance, for $b_1 < 0, b_2 > 0$, $(\phi^*, A^*) \in \mathcal{S}_0 \iff A^* > A_0(\phi^*)$, and one would show that

$$B(\phi) := \frac{A_0(\phi)}{A_1(\phi)} \geq 1$$

and, since $A_1(\phi) < 0$, this implies that $A_0(\phi) \leq A_1(\phi)$, from where the result follows.

Lemma A.3. Let $\omega_{\text{high}} \in \mathbb{R}_+$ such that $0 < \omega < \omega_{\text{high}}$, and let

$$\mathcal{S}'_0 := \{(\phi, A) : \omega - \omega_{\text{high}} - Ab_1 \sin(\phi) < 0\},$$

$$\mathcal{S}_2 := \{(\phi, A) : A'_1(\phi) < A < A'_2(\phi)\},$$

where

$$A'_1 = \frac{2(\omega - \omega_{\text{high}}) \left(b_2 \cos(\phi) - b_1 \sin(\phi) - \sqrt{b_2^2 + b_1^2} \right)}{(b_1 \cos(\phi) + b_2 \sin(\phi))^2},$$

$$A'_2 = \frac{2(\omega - \omega_{\text{high}}) \left(b_2 \cos(\phi) - b_1 \sin(\phi) + \sqrt{b_2^2 + b_1^2} \right)}{(b_1 \cos(\phi) + b_2 \sin(\phi))^2}.$$

Then

$$\mathcal{S}_2 \subset \mathcal{S}'_0.$$

Proof. The proof is identical to that of Lemma A.1 and will therefore be omitted. \square

Lemma A.4. Define

$$\mathcal{S}_m := \{(\phi, A) : 1/2 Ab_1 \cos(\phi) + \sigma + 1/2 Ab_2 \sin(\phi) < 0\}$$

and

$$M(\theta, \phi, A) := e^{2\omega_{\text{high}}^{-1} \int_0^\theta g(z, \phi, A) dz},$$

where $0 < \omega < \omega_{\text{high}}$, and

$$g(\theta, \phi, A) := \sigma + (\cos(\theta) b_1 + \sin(\theta) b_2) A (\cos(\phi) \cos(\theta) + \sin(\phi) \sin(\theta)).$$

If $(A^*, \phi^*) \in \mathcal{S}_m$, then

$$\lim_{\theta \rightarrow \infty} M(\theta, \phi^*, A^*) = 0$$

and $\exists C_4, C_5 \in \mathbb{R}_+$ such that

$$0 < C_4 \leq \lim_{\theta \rightarrow \infty} \int_0^\theta M(y, \phi^*, A^*) dy \leq C_5.$$

Proof. First observe that for given A and ϕ , $M(\theta, \phi, A)$ is positive for all θ by its definition, and so is $\int_0^\theta M(y, \phi^*, A^*) dy$. Next, we evaluate the integral

$$\begin{aligned} \int_0^\theta g(z, \phi, A) dz &= \int_0^\theta \sigma + (\cos(z) b_1 + \sin(z) b_2) A (\cos(\phi) \cos(z) + \sin(\phi) \sin(z)) dz \\ &= (1/2 Ab_1 \cos(\phi) + \sigma + 1/2 Ab_2 \sin(\phi)) \theta + \varphi(\theta, \phi, A), \end{aligned}$$

where

$$\begin{aligned}\varphi(\theta, \phi, A) &= 1/2 Ab_1 \sin(\phi) + 1/2 Ab_2 \cos(\phi) - 1/2 A (\cos(\theta))^2 b_2 \cos(\phi) \\ &\quad + 1/2 Ab_1 \cos(\phi) \cos(\theta) \sin(\theta) - 1/2 A (\cos(\theta))^2 b_1 \sin(\phi) \\ &\quad - 1/2 Ab_2 \sin(\phi) \cos(\theta) \sin(\theta).\end{aligned}$$

Since $|\sin(\phi)| \leq 1$ and $|\cos(\phi)| \leq 1$, from the above one can write

$$|\varphi(\theta, \phi, A)| \leq |1/2 Ab_1| + |1/2 Ab_2| + |1/2 Ab_2| + |1/2 Ab_1| + |1/2 Ab_1| + |1/2 Ab_2| =: C_1,$$

where $C_1 \in \mathbb{R}_+$. Therefore,

$$\begin{aligned}M(\theta, \phi, A) &= e^{2\omega_{\text{high}}^{-1} \int_0^\theta g(z, \phi, A) dz}, \\ M(\theta, \phi, A) &= e^{2\omega_{\text{high}}^{-1} ((1/2 Ab_1 \cos(\phi) + \sigma + 1/2 Ab_2 \sin(\phi))\theta + \varphi(\theta, \phi, A))}.\end{aligned}$$

Utilizing $|\varphi| \leq C_1$, one gets

$$e^{(1/2 Ab_1 \cos(\phi) + \sigma + 1/2 Ab_2 \sin(\phi))\theta} C_2 \leq M(\theta, \phi, A) \leq e^{(1/2 Ab_1 \cos(\phi) + \sigma + 1/2 Ab_2 \sin(\phi))\theta} C_3, \quad (35)$$

where $C_2 := e^{-2\omega_{\text{high}}^{-1} C_1}$, $C_3 := e^{2\omega_{\text{high}}^{-1} C_1}$, and $C_2, C_3 \in \mathbb{R}_+$. Thus, if $(\phi^*, A^*) \in \mathcal{S}_m$, we will have

$$(1/2 A^* b_1 \cos(\phi^*) + \sigma + 1/2 A^* b_2 \sin(\phi^*))\theta < 0,$$

which implies from equation 35 that $M(\theta, \phi^*, A^*) \rightarrow 0$ as $\theta \rightarrow \infty$, which proves the first claim of the lemma.

For the second statement, note that

$$C_2 \int_0^\theta e^{(1/2 Ab_1 \cos(\phi) + \sigma + 1/2 Ab_2 \sin(\phi))y} dy \leq \int_0^\theta M(y, \phi, A) dy = \int_0^\theta e^{2\omega_{\text{high}}^{-1} \int_0^y g(z, \phi, A) dz} dy.$$

The lower bound can be written as

$$\begin{aligned}& C_2 \int_0^\theta e^{(1/2 Ab_1 \cos(\phi) + \sigma + 1/2 Ab_2 \sin(\phi))y} dy \\ &= C_2 (1/2 Ab_1 \cos(\phi) + \sigma + 1/2 Ab_2 \sin(\phi))^{-1} e^{(1/2 Ab_1 \cos(\phi) + \sigma + 1/2 Ab_2 \sin(\phi))y} \Big|_0^\theta \\ &= C_4 (1 - e^{(1/2 Ab_1 \cos(\phi) + \sigma + 1/2 Ab_2 \sin(\phi))\theta}),\end{aligned}$$

where $C_4 := -C_2 (1/2 Ab_1 \cos(\phi) + \sigma + 1/2 Ab_2 \sin(\phi))^{-1}$. Thus,

$$C_4 (1 - e^{(1/2 Ab_1 \cos(\phi) + \sigma + 1/2 Ab_2 \sin(\phi))\theta}) \leq \int_0^\theta M(y, \phi, A) dy. \quad (36)$$

Similarly,

$$\int_0^\theta M(y, \phi, A) dy = \int_0^\theta e^{2\omega_{\text{high}}^{-1} \int_0^y g(z, \phi, A) dz} dy \leq C_3 \int_0^\theta e^{(1/2 Ab_1 \cos(\phi) + \sigma + 1/2 Ab_2 \sin(\phi))y} dy.$$

The upper bound can be written as

$$\begin{aligned} & C_3 \int_0^\theta e^{(1/2 Ab_1 \cos(\phi) + \sigma + 1/2 Ab_2 \sin(\phi))y} dy \\ &= C_3 (1/2 Ab_1 \cos(\phi) + \sigma + 1/2 Ab_2 \sin(\phi))^{-1} e^{(1/2 Ab_1 \cos(\phi) + \sigma + 1/2 Ab_2 \sin(\phi))y} \Big|_0^\theta \\ &= C_5 (1 - e^{(1/2 Ab_1 \cos(\phi) + \sigma + 1/2 Ab_2 \sin(\phi))\theta}), \end{aligned} \quad (37)$$

where $C_5 := -C_3 (1/2 Ab_1 \cos(\phi) + \sigma + 1/2 Ab_2 \sin(\phi))^{-1}$. Thus,

$$\int_0^\theta M(y, \phi, A) dy \leq C_5 (1 - e^{(1/2 Ab_1 \cos(\phi) + \sigma + 1/2 Ab_2 \sin(\phi))\theta}).$$

If $(\phi^*, A^*) \in \mathcal{S}_m$, we will have $(1/2 A^* b_1 \cos(\phi^*) + \sigma + 1/2 A^* b_2 \sin(\phi^*))\theta < 0$, which implies from equations 36 and 37 that

$$C_4 \leq \int_0^\theta M(y, \phi^*, A^*) dy \leq C_5$$

as $\theta \rightarrow \infty$. Note that $C_4, C_5 \in R_+$ since $(\phi^*, A^*) \in \mathcal{S}_m$ and $C_2 \in R_+$. Hence follows the second claim of the lemma. \square

B. Connections and Comparisons with Phase Averaging

In this section we comment on the connections between the main results obtained in Section 3 and the phase-averaging approach, which has been used in a number of fluid flow studies for the analysis of oscillations (Noack et al., 2003; Tadmor et al., 2003; Noack et al., 2004; Tadmor et al., 2004; Rowley and Juttijudata, 2005). We will consider a simple example and provide a comparison through this example.

Consider the fluid flow problem described in Section 2 and suppose that model reduction and simplification yield the closed-loop oscillatory mode dynamics 9–10, where $\sigma = 2$, $\alpha = 1$, $\omega = 6$, $b_1 = 1$, and $b_2 = 3$. Let the system be subject to the initial condition $a_0 = [1 \ 1]$, or equivalently $r_0 = \sqrt{2}$ and $\omega_0 = 45^\circ = \pi/4$, and frequency constraints $\omega_{\text{low}} = 4$ and $\omega_{\text{high}} = 15$. The unforced response of the system ($A = 0$) is shown in Figure 8. It can be seen that the system reaches a limit cycle of amplitude $\sqrt{\sigma/\alpha} = \sqrt{2} = 1.4142$ and keeps oscillating at a frequency $\omega = 6$. The control objective is to choose controller parameters A and ϕ so as achieve $r \rightarrow 0$ while keeping the frequency between $\omega_{\text{low}} = 4$ and $\omega_{\text{high}} = 15$. We will first utilize techniques developed in Section 3 and then perform a comparison with the phase-averaging method.

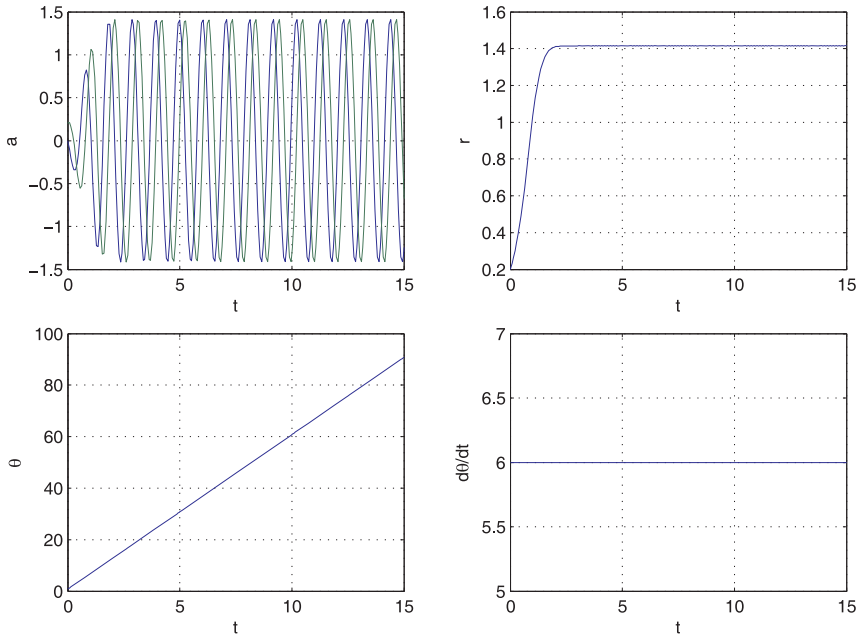


Figure 8. Unforced response of the system.

We first look at the values that A and ϕ can take based on the frequency criterion $\omega_{\text{low}} < \omega < \omega_{\text{high}}$. It was derived in Theorem 3.1 that the control parameters (ϕ, A) must lie in $\mathcal{S}_f = \mathcal{S}_1 \cap \mathcal{S}_2$, where \mathcal{S}_1 and \mathcal{S}_2 are as given in the theorem statement. We also need to determine the conditions under which the magnitude criterion $r \rightarrow 0$ is achieved. These conditions were derived in Theorem 3.2, which require that $(\phi, A) \in \mathcal{S}_m$. For the system considered in this example, the frequency and magnitude conditions are plotted in Figure 9. The figure shows the boundaries for the satisfaction of the frequency criterion and the boundaries for the satisfaction of the magnitude criterion. In the notation of Theorems 3.1 and 3.2, the zone in the (ϕ, A) plane where the frequency criterion is satisfied is termed \mathcal{S}_f and the zone where the magnitude criterion is satisfied is termed \mathcal{S}_m . In the figure the zone \mathcal{S}_f appears red and the zone \mathcal{S}_m appears green. The control parameters we seek are those that satisfy both criteria, which corresponds to the intersection of the red and green zones. This intersection zone $\mathcal{S}_f \cap \mathcal{S}_m$ appears as the mixture of red and green, i.e. brown.³ The point $(\phi, A) = (110^\circ, -2.5)$, which is marked with a circle in the figure, lies in this region and we can therefore use these parameter values for the control law, i.e. $\gamma = -2.5r \cos(\theta - 110\pi/180)$. Figure 10 shows the controlled response of the system, where the controller is turned on at $t = 5$ s. It can be seen from the figure that the designed control achieves the desired task and drives $r \rightarrow 0$, in addition to keeping $\dot{\theta}$ between $\omega_{\text{low}} = 4$ and $\omega_{\text{high}} = 15$.

We now proceed with an analysis based on phase averaging, where one approximates the system 12–13 with an averaged system obtained by averaging the right-hand side of equations 12–13 over $\theta \in (0, 2\pi)$. The resulting averaged system is of the form

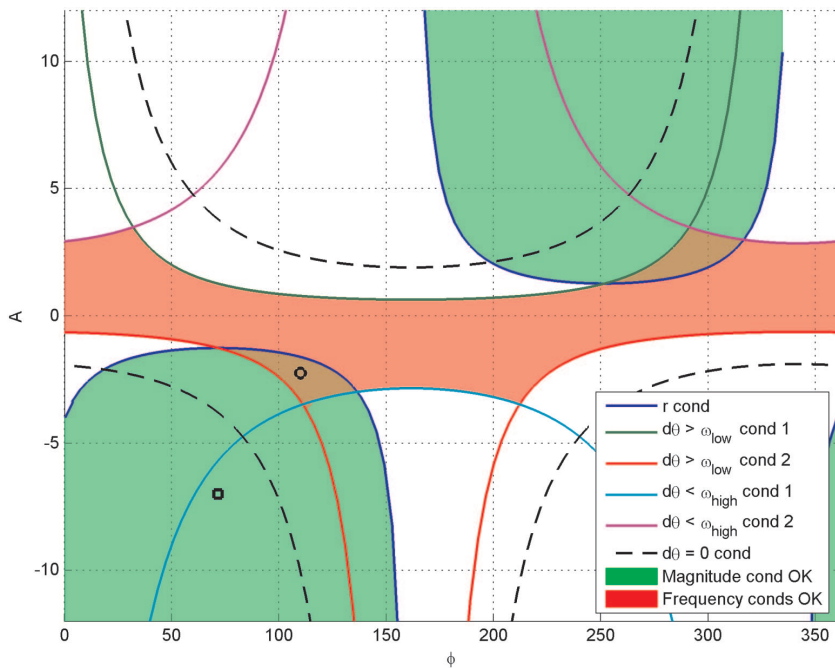


Figure 9. Frequency and magnitude conditions for controller parameter values A and ϕ .

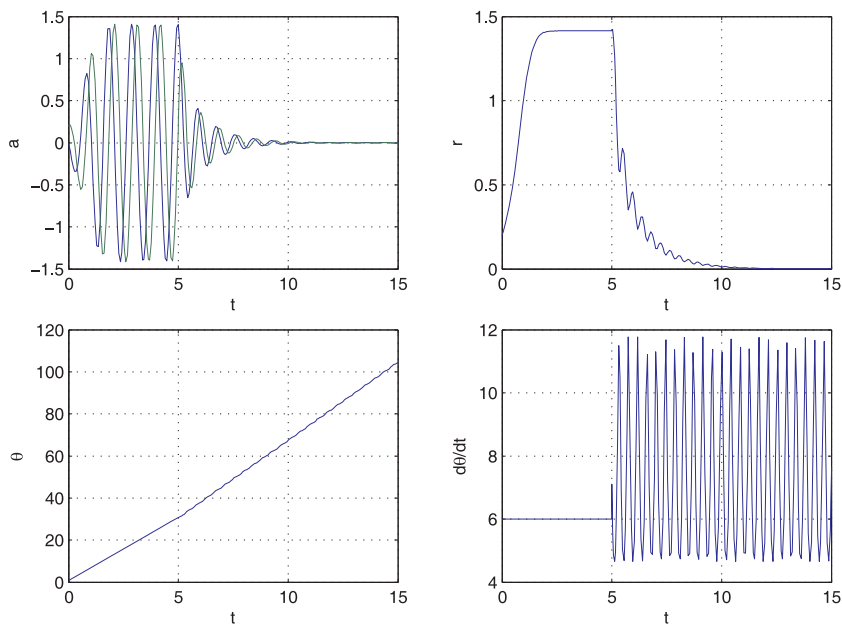


Figure 10. Response of the system under controller design based on the results in Section 3.

$$\dot{r} = (\sigma + A/2(b_1 \cos(\phi) + b_2 \sin(\phi)))r - \alpha r^3 = (\sigma + A/2 \langle b, 1_\phi \rangle) - \alpha r^3 \quad (38)$$

$$\dot{\theta} = \omega + A/2(b_2 \cos(\phi) - b_1 \sin(\phi)) = \omega + A/2 \langle b_\perp, 1_\phi \rangle, \quad (39)$$

where

$$b = \begin{bmatrix} b_1 \\ b_2 \end{bmatrix}, \quad b_\perp := \begin{bmatrix} b_2 \\ -b_1 \end{bmatrix}, \quad 1_\phi := \begin{bmatrix} \cos(\phi) \\ \sin(\phi) \end{bmatrix}$$

and $\langle \cdot, \cdot \rangle$ is the dot product operation. It can be observed from equations 38–39 above that the best choice for ϕ is $\phi = \angle b$, since in that case the term $\langle b, 1_\phi \rangle$ is maximized, so the control has maximum effect on r , and the term $\langle b_\perp, 1_\phi \rangle$ vanishes, so there is no change in the frequency ω . This choice for ϕ results in the averaged dynamics

$$\dot{r} = (\sigma + A/2\|b\|) - \alpha r^3, \quad (40)$$

$$\dot{\theta} = \omega, \quad (41)$$

from which one can see that for any choice of A such that $A < -2\sigma/\|b\| = -1.2649$, the origin of system 40–41 is globally attractive and the attraction gets stronger as A becomes more negative. Moreover, the averaged system 38–39 suggests that the frequency is unchanged by the choice of A and will always be ω , and hence $\dot{\theta}$ will always stay within the limits ω_{low} and ω_{high} . In the light of this discussion, we may pick $A = -7$ and $\phi = \angle b = 45^\circ = \pi/4$ so that $\gamma = -7 \cos(\theta - \pi/4)$. The response of the resulting closed-loop Galerkin system is shown in Figure 11. Contrary to the prediction of system 38–39, the controller does not achieve either $r \rightarrow 0$ or $\omega_{\text{low}} < \omega$ (observe that $4 \not\prec \omega$ for $t > 5.5$). We may utilize the results derived in Section 3 to understand why the phase-averaging analysis fails in this case. Let us look at Figure 9 again, and in particular at the point $(\phi, A) = (45^\circ, -7)$, which is marked with a square in the figure. We first observe that the square lies outside the red zone corresponding to \mathcal{S}_f , which explains why the frequency criterion $\omega_{\text{low}} < \omega < \omega_{\text{high}}$ is not satisfied. One observes, however, that whether r will converge to zero in the averaged system 38–39 is dictated by the negativity of the coefficient of r , i.e. $(\sigma + A/2(b_1 \cos(\phi) + b_2 \sin(\phi))) < 0$. This inequality is identical to the rule defining the set \mathcal{S}_m in Theorem 3.2. Therefore, it is curious that despite the condition for stabilizing the averaged system 38–39 being the same as the condition for the satisfaction of the magnitude criterion, and although this condition is satisfied for the choice $(\phi, A) = (45^\circ, -7)$, this still does not result in $r \rightarrow 0$ in the original system. To shed light on this situation, let us make an additional observation by looking at the curves corresponding to $\omega_{\text{low}} = 0$ in equation 18 under Theorem 3.1, which are shown as dashed lines in Figure 9. The region bounded by the dashed lines corresponds to (ϕ, A) that will ensure that $\dot{\theta} > 0$ at all times. One sees that the point $(\phi, A) = (45^\circ, -7)$ in the figure lies outside this region, meaning that there exists a value of θ_s such that $\dot{\theta}|_{\theta=\theta_s} = 0$. Since $\dot{\theta}$ is only dependent on θ , this implies that once $\theta = \theta_s$, it will remain constant. This can also be seen from Figure 11, where it is observed that at around $t = 5.3$, θ reaches a value of about 30.58 and remains at that value thereafter. This fails a key assumption used in the analysis in Theorem 3.2, which is the existence of an invertible transformation χ such that $\theta = \chi(t)$.

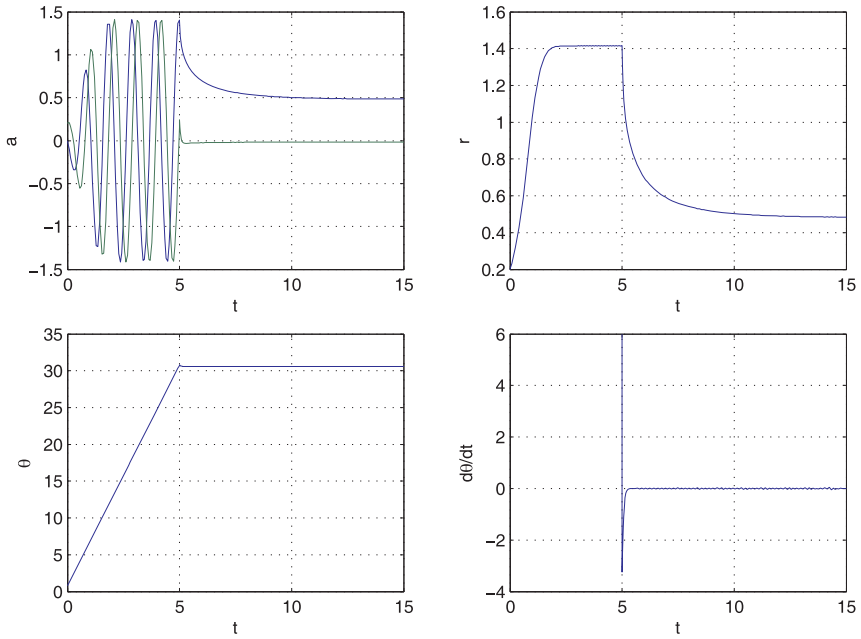


Figure 11. Response of the system under controller design based on phase averaging.

Therefore, the result obtained in Theorem 3.2, and also the result of phase-averaging analysis, do not apply. In fact, once $\theta = \theta_s$, θ remains constant and so the dynamics for r become

$$\dot{r} = \sigma' r - \alpha r^3, \quad (42)$$

where

$$\sigma' := g(\theta_s, \phi, A) = (\sigma + (\cos(\theta_s) b_1 + \sin(\theta_s) b_2) A (\cos(\phi) \cos(\theta_s) + \sin(\phi) \sin(\theta_s)))$$

is a constant. Dividing both sides of equation 42 by $1/r^3$ and letting $s = 1/r^2$ yields

$$\dot{s} = -2\sigma' s + 2\alpha.$$

Solving and transforming back to r gives

$$r^2(t) = \frac{\sigma' r_0^2}{(\sigma' - \alpha)e^{-2\sigma' t} + \alpha r_0^2} = \frac{g(\theta_s, \phi, A) r_0^2}{(g(\theta_s) - \alpha)e^{-2g(\theta_s, \phi, A)t} + \alpha r_0^2}.$$

This result further clarifies why phase-averaging analysis does not work for this case: the expression above depends on the value of g at only a single point θ_s and therefore looking at $\int_0^{2\pi} g(z, \phi, A) dz$, the integral over the range $(0, 2\pi)$, is not meaningful.

The discussion above can be generalized to obtain the following corollary on the validity of phase-averaging-based analyses.

Corollary B.1. Consider the fluid flow problem in Section 2, and the evolution equation for the oscillatory modes under the control $\gamma = A^*r \cos(\theta - \phi^*)$ given in equations 9–10. Also, consider the system resulting from averaging this system over $\theta \in (0, 2\pi)$, which is

$$\dot{r} = (\sigma + A^*/2(b_1 \cos(\phi^*) + b_2 \sin(\phi^*)))r - ar^3, \quad (43)$$

$$\dot{\theta} = \omega + A^*/2(b_2 \cos(\phi^*) - b_1 \sin(\phi^*)). \quad (44)$$

Assume that $(\phi^*, A^*) \in \mathcal{S}_c$, where

$$\mathcal{S}_c := \{(\phi, A) : A_{c1}(\phi) < A < A_{c2}(\phi)\}$$

and

$$A_{c1}(\phi) = \frac{2\omega \left(b_2 \cos(\phi) - b_1 \sin(\phi) - \sqrt{b_2^2 + b_1^2} \right)}{(b_1 \cos(\phi) + b_2 \sin(\phi))^2}, \quad (45)$$

$$A_{c2}(\phi) = \frac{2\omega \left(b_2 \cos(\phi) - b_1 \sin(\phi) + \sqrt{b_2^2 + b_1^2} \right)}{(b_1 \cos(\phi) + b_2 \sin(\phi))^2}. \quad (46)$$

In this case, if $r \rightarrow 0$ in the averaged system 43–44, then $r \rightarrow 0$ in the original system 9–10.

Proof. The proof follows immediately from those of Theorems 3.1 and 3.2 as follows: first note that equations 45–46 are obtained by letting $\omega_{\text{low}} = 0$ in equations 18 and 19 under Theorem 3.1, and therefore they ensure that $\dot{\theta} > 0$ for the closed-loop system 12–13. Thus, θ is strictly increasing in time and one can map the time t to angle values θ with a one to one and onto function χ such that $\theta = \chi(t)$. Proceeding identically to the proof of Theorem 3.2, one sees that $r \rightarrow 0$ will be achieved if $(\phi^*, A^*) \in \mathcal{S}_m := \{(\phi, A) : 1/2 Ab_1 \cos(\phi) + \sigma + 1/2 Ab_2 \sin(\phi) < 0\}$. But, if $r \rightarrow 0$ in the averaged system, this means that we have the coefficient of r negative, i.e. $\sigma + A^*/2(b_1 \cos(\phi^*) + b_2 \sin(\phi^*)) < 0$, which is the same as $(\phi^*, A^*) \in \mathcal{S}_m$. Hence follows the result of the corollary. \square

NOTE

1. These equations have been nondimensionalized by scaling \mathbf{u} by the free-stream velocity U_∞ , the local speed of sound by the ambient sound speed $c_\infty = (\kappa RT_\infty)^{1/2}$, where T_∞ is the ambient temperature, the Cartesian coordinates \mathbf{x} by the cavity depth D , time by D/U_∞ , and pressure by $\bar{\rho}U_\infty^2$, where $\bar{\rho}$ denotes mean density.
2. When printed in gray scale, green appears light, red appears dark, and brown appears slightly darker.
3. When printed in gray scale, green appears light, red appears dark, and brown appears slightly darker.

REFERENCES

- Aamo, O. M., Krstic, M. and Bewley, T. R., 2003, "Control of mixing by boundary feedback in 2d channel flow," *Automatica* **39**(9), 1597–1606.
- Amitay, M., Smith, D. R., Kibens, V., Parekh, D. E. and Glezer, A., 2001, "Aerodynamic flow control over an unconventional airfoil using synthetic jet actuators," *AIAA Journal* **39**(3), 361–370.
- Banaszuk, A., Ariyur, K. B., Krstic, M. and Jacobson, C. A., 2004, "An adaptive algorithm for control of combustion instability," *Automatica* **40**(11), 1965–1972.
- Baramov, L., Tutty, O. R. and Rogers, E., 2004, " h_∞ control of non-periodic two-dimensional channel flow," *IEEE Transactions on Control Systems Technology* **12**(1), 111–122.
- Bewley, T. R., 2001, "Flow control: new challenges for a new Renaissance," *Progress in Aerospace Sciences* **37**(1), 21–58.
- Camphouse, R. C., 2005, "Boundary feedback control using proper orthogonal decomposition models," *Journal of Guidance, Control, and Dynamics* **28**, 931–938.
- Caraballo, E., Little, J., Debiasi, M. and Samimy, M., 2007, "Development and implementation of an experimental based reduced-order model for feedback control of subsonic cavity flows," *Journal of Fluids Engineering* **129**, 813–824.
- Cohen, K., Siegel, S., McLaughlin, T., Gillies, E. and Myatt, J., 2005, "Closed-loop approaches to control of a wake flow modeled by the Ginzburg–Landau equation," *Computers and Fluids* **34**(8), 927–949.
- Cortezzi, L., Speyer, J. L., Lee, K. H. and Kim, J., 1998, "Robust reduced-order control of turbulent channel flows via distributed sensors and actuators," in *Proceedings of the 37th IEEE Conference on Decision and Control*, Tampa, FL, 1998.
- Efe, M. O. and Ozbay, H., 2004, "Low dimensional modelling and Dirichlet boundary controller design for Burgers equation," *International Journal of Control* **77**(10), 895–906.
- Fitzpatrick, K., Feng, Y., Lind, R., Kurdila, A. J. and Mikolaitis, D. W., 2005, "Flow control in a driven cavity incorporating excitation phase differential," *Journal of Guidance, Control, and Dynamics* **28**(1), 63–70.
- Gad-el Hak, M., 2000, *Flow Control – Passive, Active, and Reactive Flow Management*, Cambridge University Press, New York.
- Graham, W. R., Peraire, J. and Tang, K. Y., 1999, "Optimal control of vortex shedding using low-order models I – open-loop model development," *International Journal for Numerical Methods in Engineering* **44**, 945–972.
- Gilarranz, J. L., Traub, L. W. and Rediniotis, O. K., 2005, "A new class of synthetic jet actuators: Part II: Application to flow separation control," *Journal of Fluids Engineering* **127**(2), 377–387.
- Hinze, M. and Kunisch, K., 2004, "Second order methods for boundary control of the instationary Navier–Stokes system," *Zeitschrift für Angewandte Mathematik und Mechanik* **84**(3), 171–187.
- Hogberg, M., Bewley, T. R. and Henningson, D. S., 2001, "Linear feedback control and estimation of transition in plane channel flow," *Journal of Fluid Mechanics* **481**, 149–175.
- Holmes, P., Lumley, J. L. and Berkooz, G., 1996, *Turbulence, Coherent Structures, Dynamical Systems, and Symmetry*, Cambridge University Press, Cambridge.
- Jordan, D. W., and Smith, P., 1999, *Nonlinear Ordinary Differential Equations: An Introduction to Dynamical Systems*. Oxford University Press, Oxford.
- Joslin, R. D., 1998, Aircraft laminar flow control. *Annual Review of Fluid Mechanics* **30**, 1–29.
- Kasnakoglu, C. and Serrani, A., 2007, "Attenuation of oscillations in Galerkin systems using center-manifold techniques," *European Journal of Control* **13**(5), 529.
- Kasnakoglu, C., Serrani, A. and Efe, M. O., 2008, "Control input separation by actuation mode expansion for flow control problems," *International Journal of Control* **81**(9), 1475–1492.
- Kim, J., 2003, "Control of turbulent boundary layers," *Physics of Fluids* **15**, 1093.
- Kobayashi, T. and Oya, M., 2003, "Nonlinear boundary control of coupled Burgers' equations," *Control and Cybernetics* **32**(2), 245–258.
- Krstic, M., 1999, "On global stabilization of Burgers' equation by boundary control," *Systems and Control Letters* **37**(3), 123–141.
- Landau, L. D. and Lifshitz, E. M., 1987, *Course of Theoretical Physics, vol. 6: Fluid Mechanics*. Pergamon Press, Oxford.
- Noack, B. R., Afanasiev, K., Morzynski, M., Tadmor, G. and Thiele, F., 2003, "A hierarchy of low-dimensional models for the transient and post-transient cylinder wake," *Journal of Fluid Mechanics* **497**, 335–363.

- Noack, B. R. and Eckelmann, H., 1994, "A global stability analysis of the steady and periodic cylinder wake," *Journal of Fluid Mechanics* **270**, 297–330.
- Noack, B. R., Papas, P. and Monkewitz, P. A., 2005, "The need for a pressure-term representation in empirical Galerkin models of incompressible shear flows," *Journal of Fluid Mechanics* **523**, 339–365.
- Noack, B. R., Tadmor, G. and Morzynski, M., 2004, "Low-dimensional models for feedback flow control. Part I: Empirical Galerkin models," in *Proceedings of the 2nd AIAA Flow Control Conference*, Portland, OR, 2004. AIAA Paper 2004-2408.
- Oleschuk, R., Westra, K., Harrison, D. J., Edmonton, A. and Microelectronic, A., 2000, "Electrokinetic control of fluid flow in native poly (dimethylsiloxane) capillary electrophoresis devices," *Electrophoresis* **21**, 107–115.
- Park, H. M. and Lee, M. W., 2000, "Boundary control of the Navier–Stokes equation by empirical reduction of modes," *Computer Methods in Applied Mechanics and Engineering* **188(1–3)**, 165–186.
- Rowley, C. W., Colonius, T. and Murray, R. M., 2004, "Model reduction for compressible flows using POD and Galerkin projection," *Physica D* **189(1–2)**, 115–129.
- Rowley, C. W. and Juttijudata, V., 2005, "Model-based control and estimation of cavity flow oscillations," in *Proceedings of the 44th IEEE Conference on Decision and Control*, Seville, Spain, 2005.
- Rowley, C. W. and Marsden, J. E., 2000, "Reconstruction equations and the Karhunen–Loeve expansion for systems with symmetry," *Physica D* **142(1–2)**, 1–19.
- Samimy, M., Debiasi, M., Caraballo, E., Serrani, A., Yuan, X., Little, J. and Myatt, J. H., 2007, "Feedback control of subsonic cavity flows using reduced-order models," *Journal of Fluid Mechanics* **579**, 315–346.
- Seiler, K., Fan, Z. H., Fluri, K. and Harrison, D. J., 1994, "Electroosmotic pumping and valveless control of fluid flow within a manifold of capillaries on a glass chip," *Analytical Chemistry* **66(20)**, 3485–3491.
- Singh, S. N., Myatt, J. H., Addington, G. A., Banda, S. and Hall, J. K., 2001, "Optimal feedback control of vortex shedding using proper orthogonal decomposition models," *Transactions of the ASME. Journal of Fluids Engineering* **123(3)**, 612–618.
- Sirovich, L., 1987, "Turbulence and the dynamics of coherent structures," *Quarterly Journal of Applied Mathematics* **45(3)**, 561–590.
- Smaoui, N., 2005, Boundary and distributed control of the viscous Burgers equation. *Journal of Computational and Applied Mathematics* **182(1)**, 91–104.
- Stuart, J. T., 2006, "On the non-linear mechanics of wave disturbances in stable and unstable parallel flows. Part 1. The basic behaviour in plane Poiseuille flow", *Journal of Fluid Mechanics Digital Archive* **9(3)**, 353–370.
- Tadmor, G., Noack, B. R., Dillmann, A., Gerhard, J., Pastoor, M., King, R. and Morzynski, M. 2003, "Control, observation and energy regulation of wake flow instabilities", in *Proceedings of the 42nd IEEE Conference on Decision and Control*, Maui, HI, 2003.
- Tadmor, G., Noack, B. R., Morzynski, M. and Siegel, S., 2004, "Low-dimensional models for feedback flow control. Part II: Controller design and dynamic estimation," in *Proceedings of the 2nd AIAA Flow Control Conference*, Portland, OR, 2004. AIAA Paper 2004-2409.
- Wu, J., Lu, X., Denny, A. G., Fan, M. and Wu, J. M., 1998, "Post-stall flow control on an airfoil by local unsteady forcing," *Journal of Fluid Mechanics* **371**, 21–58.